



Simultaneous non-contrast angiography and intraplaque haemorrhage (SNAP) imaging for cervical artery dissections

R.J. Huang, Y. Lu, M. Zhu, J.F. Zhu, Y.G. Li*

Radiology Department, The First Affiliated Hospital of Soochow University, Shizi Street 188#, Suzhou, Jiangsu Province, 215006, PR China

ARTICLE INFORMATION

Article history:

Received 4 March 2019

Accepted 26 June 2019

AIM: To evaluate the feasibility of high-resolution magnetic resonance imaging (MRI) with a simultaneous non-contrast angiography and intraplaque haemorrhage (SNAP) sequence in identifying cervical artery dissections (CeAD).

MATERIALS AND METHODS: Fifty-three patients with suspected CeAD underwent the SNAP sequence (including non-contrast magnetic resonance angiography [MRA] and heavy T1-weighting vessel wall images simultaneously in a single scan) and conventional MRI sequences (including three-dimensional [3D] time-of-flight MRA and T1-weighted black-blood imaging [T1W BB]) and cervical vascular ultrasound (CVUS). In diagnosis of CeAD, the diagnostic sensitivity and specificity of SNAP, and the diagnostic coherence between SNAP and conventional sequences and between SNAP and CVUS was analysed. At follow-up, the absolute signal (AS) and signal index (SI) of the intramural haematoma (IMH) between vessel wall images on SNAP and T1W-BB images were compared. The image quality of SNAP was analysed by comparing the signal-to-noise ratio (SNR) between vessel wall images from the SNAP and T1W-BB sequences.

RESULTS: The SNAP sequence was found to provide good performance in the diagnosis of CeAD (sensitivity 72.2%, specificity 98.2%); good agreement was found between SNAP and conventional sequences (Cohen's $\kappa=0.76$, $p<0.05$); and excellent agreement was found between SNAP and CVUS (Cohen's $\kappa=0.83$, $p<0.05$). There was no significant difference between AS or SI of the IMH of the vessel wall images within the SNAP and T1W-BB sequences during the review. The SNAP sequence had higher SNR of the IMH compared to T1W-BB, T2W-BB, proton-density-weighted volume isotropic turbo-spin-echo acquisition imaging (PD-VISTA) sequences ($p<0.05$).

CONCLUSION: The SNAP sequence holds the potential to be preferred choice for screening of patients with a high suspicion of CeAD and for the follow-up of IMH after treatment.

© 2019 The Royal College of Radiologists. Published by Elsevier Ltd. All rights reserved.

* Guarantor and correspondent: Y.G. Li, Radiology Department, The First Affiliated Hospital of Soochow University, Shizi Street 188#, Suzhou, Jiangsu Province, 215006, PR China. Tel.: +86 512 67780155; fax: +86 512 67780633.

E-mail address: liyonggang224@163.com (Y.G. Li).

Introduction

Cervicocranial artery dissections (CeAD), including carotid and vertebral artery dissections, which are a major

cause of ischaemic stroke in young and middle-aged adults, have been estimated to have an annual incidence of 1–1.5 per 100,000 persons, with extracranial segments more prone to dissection than intracranial segments.^{1–3} CeAD are further classified as spontaneous or traumatic.^{3,4} The former is more likely to be ignored by patients and may lead to adverse consequences. CeAD of one or both side can appear as cerebral ischaemia, stroke, blindness, subarachnoid haemorrhage (SAH), or death.³ Early and accurate diagnosis of this disorder are therefore of great importance.

Angiographic imaging methods, such as cervical vascular ultrasound (CVUS), computed tomography angiography (CTA), magnetic resonance angiography (MRA), and digital subtraction angiography (DSA), play important roles in the diagnosis of CeAD.^{5–9} As DSA creates a luminal image based on contrast medium filling, it cannot always define intramural lesions.¹⁰ High-resolution magnetic resonance imaging (HRMRI) is increasingly regarded as the most important evidence for a diagnosis of CeAD, because it can not only provide information regarding luminal narrowing or occlusion, but can also detect intramural haematoma (IMH) as well as intimal flaps. Black-blood (BB) imaging is suitable for acquiring precise information on the luminal configuration due to its capacity to suppress flow signals and their artefacts, and is able to reveal vessel wall and lumen abnormalities; however, HRMRI is not the first choice of clinicians because of cost, long examination times, and limited coverage.

Recently, a novel HRMRI fast sequence, named simultaneous non-contrast angiography and intraplaque haemorrhage (SNAP) was developed for imaging of cervicocranial artery diseases.^{9,11–15} The SNAP sequence produces both lumen MRA images and vessel wall BB images in a single acquisition. Based on heavy T1-weighting of its vessel wall image, the SNAP sequence is quite sensitive to IMH as well as intraplaque haemorrhage.⁹ The SNAP sequence was found to provide comparable lumen size measurements and plaque characteristics to MRI in some studies,^{11,12,14,15} but previous articles regarding the SNAP sequence have rarely focused on the application of CeAD imaging. The feasibility and advantages of the SNAP sequence in CeAD diagnosis is confirmed in the present study by comparing SNAP with conventional sequences and also with CVUS. In addition, the present study confirmed the image quality of vessel wall images using the SNAP sequence in IMH by comparing these with T1-weighted BB imaging (T1W-BB) sequences. The value of the SNAP and T1W-BB sequences were also investigated in the follow-up of IMH.

Materials and methods

Participants

This study received approval from the institutional review board and written informed consent was obtained from all participants. Fifty-four patients (10 women and 44 men; mean age 41.7 years, range 31–52 years) with local symptoms indicative of CeAD (neck pain, headache, Horner

syndrome) and ischaemic symptoms (sensorimotor deficit, aphasia, amaurosis fugax) were included in the study.

CVUS and MRI

All participants underwent CVUS imaging first and then MRI. All CVUS imaging was performed by experienced neurosonographers and used a Philips CX50 high-grade ultrasonic diagnostic instrument (Bothel, WA, USA), with a 3–12 MHz broadband linear array probe and a 1–5 MHz convex array probe. Routine examination of the bilateral common carotid artery (CCA), extracranial internal carotid artery (ICA), external carotid artery (ECA), vertebral artery (VA, V1, V2, V3 segment), and subclavian artery were performed. Two-dimensional real-time imaging was used to scan the longitudinal section of the transverse section and investigate the morphology of the carotid artery and colour flow imaging. The spectrum of the arteries, the velocity of the peak systolic blood flow, the velocity of the end of diastolic blood flow, and the vascular resistance index were recorded and analysed.

All MRI imaging was performed using a 3 T MRI system (Ingenia, Philips Healthcare, Best, the Netherlands) with a eight-channel head and neck unite coil. The imaging sequences included the SNAP sequence and conventional sequences (including 3D time-of-flight (TOF) MRA and T1W-BB sequence). In addition, fat-suppressed (FS) T2W BB imaging and proton-density-weighted volume isotropic turbo-spin-echo acquisition imaging (PD-VISTA) sequences were undertaken. The parameters were as follows: 3D TOF MRA: 15 ms repetition time (TR)/3.5 ms echo time (TE); 220×128×148 mm³ field of view (FOV), 0.75×1.34×1.7 mm³ voxel size, 3.5 minutes total scanning time. T1W-BB: 20 ms TR/968 ms TE, 100×100×17 mm³ FOV, 0.8×0.8×4 mm³ voxel size, 4 minutes 58 seconds scanning time. The SNAP coronal imaging sequence (including MRA and heavy T1-weighting vessel wall images simultaneously in a single scan) was acquired with the following parameters: 10 ms TR/5 ms TE, 189×164×40 mm³ FOV, 0.8×0.8×0.8 mm³ voxel size, 4 minutes 25 seconds scanning time. FS-T2W-BB: 2,432 ms TR/40 ms TE, 100×100×15 mm³ FOV, 0.7×0.7×3.5 mm³ voxel size, 4 minutes 13 seconds scanning time. PD-VISTA: 34 ms TR/2,000 ms TE, 189×162×40 mm³ FOV, 0.6×0.6×1 mm³ voxel size, 2 minutes 40 seconds scanning time. The T1W-BB and T2W-BB sequences were acquired in the axial direction. The PD-VISTA images were acquired in the coronal direction.

Image analysis

After the conventional sequences and SNAP sequence were obtained, maximum intensity projection (MIP) of 3D TOF MRA and MRA images within the SNAP sequence were reconstructed. Multiplanar reconstruction (MPR) of vessel wall images from traditional sequences and SNAP sequence was performed. The conventional sequences were used as the reference criteria for the diagnostic performance analysis of the SNAP sequence. On conventional sequences, the evaluation focused on four separate findings: intimal flaps/

double lumen; IMHs; dilatation; pearl-and-string sign¹⁶; B-mode and colour Doppler imaging may visualise a dissection of the cervical ICA, which includes a thickened and mainly hypoechogenic vessel wall, an intimal flap, irregular artery stenosis, or a pseudoaneurysm.⁵ Blinded to clinical information and SNAP images, two reviewers with >5 years diagnostic experience of MRI or CVUS evaluated in consensus the presence or absence of dissection signs. The dissection signs on vessel wall images derived from the SNAP images were identified by other two reviewers blinded to the clinical information and conventional sequences. According to onset time, the IMH were divided into acute stage (0–3 days), subacute stage (4–60 days), and chronic stage (>60 days).¹⁷ The diagnostic sensitivity and specificity of SNAP sequences as well as CVUS in the evaluation of CeAD were analysed with the conventional sequences as the reference standard. The diagnostic coherence between the SNAP sequences and conventional sequences and between SNAP and CVUS in the diagnosis of CeAD was analysed. Absolute signal (AS, AS= signal intensity of IMH) and signal index (SI, SI=signal intensity of IMH/signal intensity

of adjacent muscles) of the IMHs on the SNAP and TIW-BB imaging were analysed initially and 3 months later respectively. The differences of AS and SI of IMH between the SNAP and T1W-BB sequences, as well as the differences of signal-to-noise ratio (SNR, SNR=signal/noise) of the IMH between the SNAP sequence and T1W-BB imaging were analysed. Region of interests (ROIs) with same area were placed in IMH and adjacent muscles, and the signal intensity as well as noise of ROIs were recorded.

Statistical analysis

The Cohen's weighted kappa was used to evaluate the agreement between the SNAP and conventional sequences as well as between the SNAP sequence and CVUS in the identification of CeAD. The paired sample *t*-test was used to compare the differences of AS and SI of IMH between SNAP sequence and T1W-BB sequence, as well as the differences of SNR between SNAP and T1W-BB. A *p*-value of <0.05 was statistically significant. Statistical calculations were conducted using SPSS 19.0 (IBM, Armonk, NY, USA). Kappa

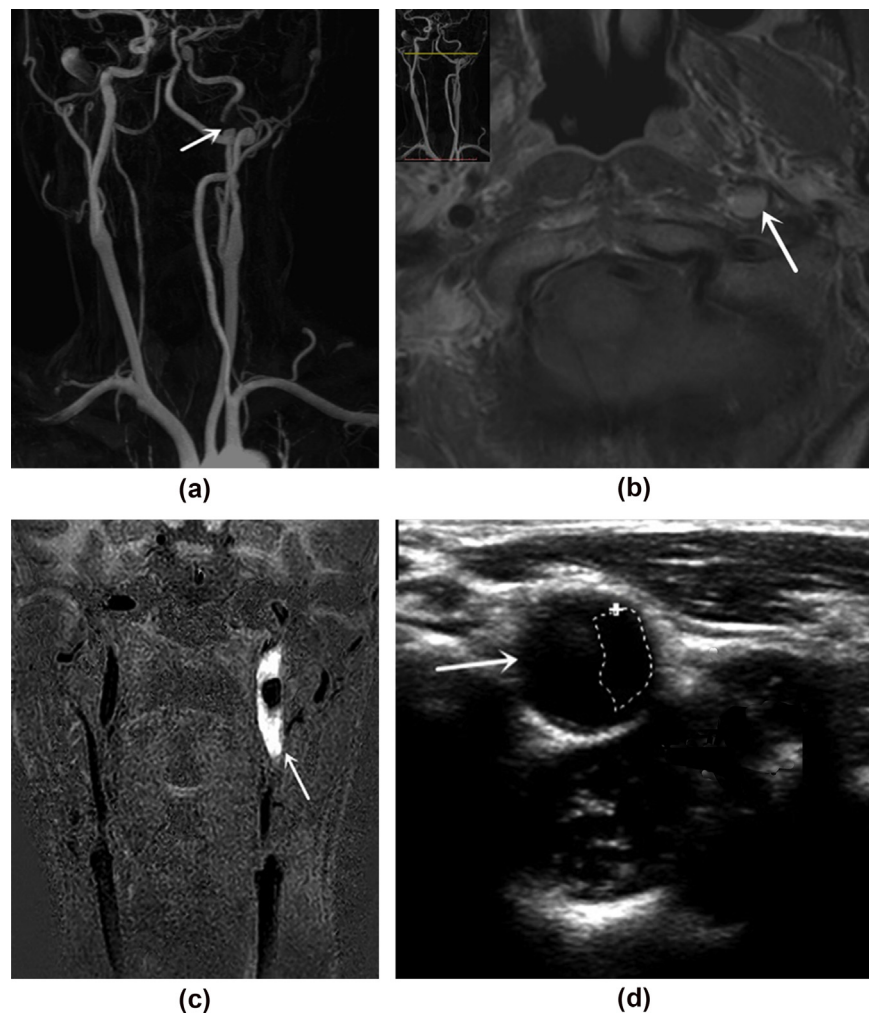


Figure 1 A 54-year-old male patient with left internal carotid artery (LICA) dissection. (a) MRA indicates local occlusion of the LICA (arrow). (b,c) The IMH showed high signal intensity on the T1W-BB image and was more obvious on the vessel wall image within SNAP (arrow). (d) On the CVUS image, the dotted area indicates the true lumen and the adjacent part was the false lumen, which was filled with low-echo IMH (arrow).

statistics were classified as follows: poor ($\kappa=0.20$); fair ($\kappa=0.21-0.40$); moderate ($\kappa=0.41-0.60$); good ($\kappa=0.61-0.80$), and excellent agreement ($\kappa=0.81-1.00$).¹⁸

Results

Seventy-five diseased arteries were found on the conventional sequences, of which 19 were diagnosed as dissection. All patients underwent HRMRI within 1 month after onset. Fourteen arteries were diagnosed with dissection on the SNAP sequence. When conventional sequences were taken as the reference standard, the SNAP sequence was found to provide good performance in the diagnosis of

IMH, with better sensitivity than CVUS (72.2% versus 68.4%) and similar specificity with CVUS (98.2% versus 98.4%). Good agreement was found between SNAP and T1W-BB (Cohen's $\kappa=0.76$, $p<0.05$) in the diagnosis of IMH (Fig 1). Eighty-one diseased arteries were found on the CVUS, of which 14 were diagnosed as dissection. Excellent agreement was found between SNAP and CVUS (Cohen's $\kappa=0.83$, $p<0.05$; Fig 1).

The AS and SI of IMH between vessel wall images within SNAP and T1W-BB at the initial examination were significantly different ($p<0.05$), and there was no significant differences in AS or SI of IMH between vessel wall images within the SNAP sequence and T1W-BB during the review 3

Table 1

Signal changes of the IMH between vessel wall images using SNAP and T1W-BB sequences (mean±standard deviation).

		SNAP	T1W-BB	p-Value
Initial examination	AS	2242.91±124.03	939.37±266.33	<0.05
	SI	1.07±0.05	2.55±0.72	<0.05
Review	AS	779.85±1076.32	139.40±198.16	0.08
	SI	0.38±0.52	0.46±0.64	0.20

IMH, intramural haematoma; SNAP, simultaneous non-contrast angiography and intraplaque haemorrhage; T1W-BB, T1-weighted black blood imaging; AS, absolute signal; SI, signal index.

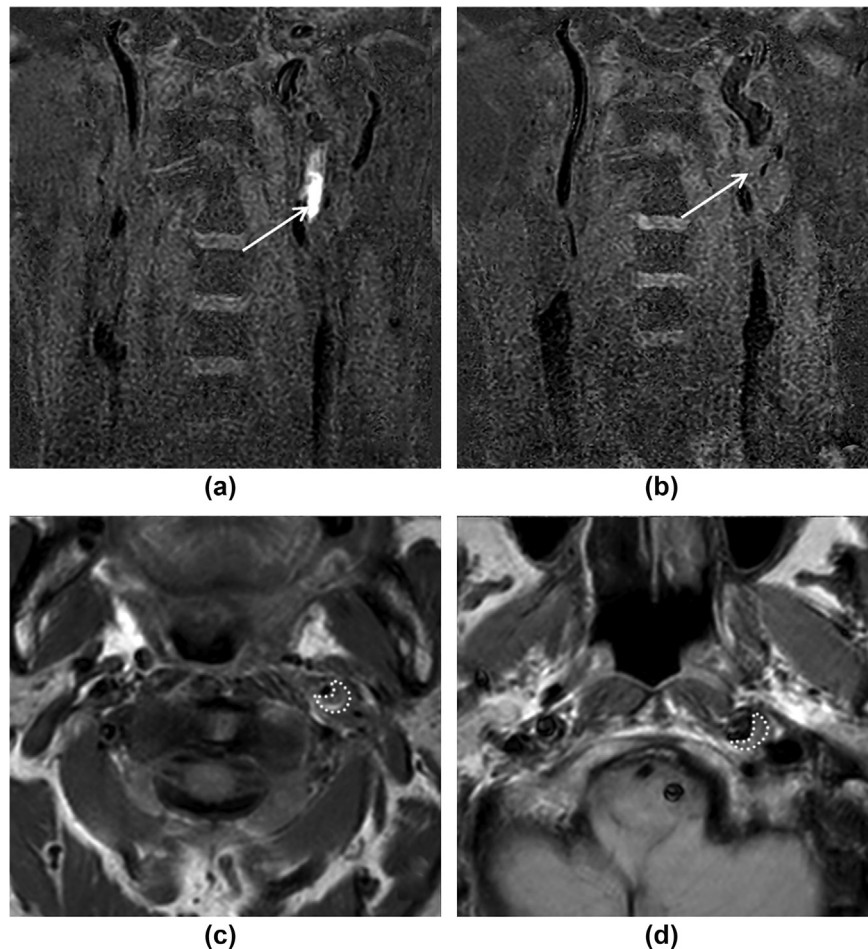


Figure 2 A 56-year-old male patient with LICA dissection was reviewed after treatment, 3-months later. Stenosis caused by IMH of the LICA in the initial vessel wall image within (a) SNAP (arrow) and (c) T1W-BB image (dotted area). (b,d) Three months later, the vessel wall image within (b) SNAP (arrow) and (d) T1W-BB image (dotted area) showed wall thickening of LICA.

Table 2

Signal changes of the IMH of vessel wall images using SNAP and T1W-BB sequences between initial examination and review (mean±standard deviation).

		Initial examination	Review	p-Value
SNAP	AS	2242.91±124.03	779.85±1076.32	<0.05
	SI	1.07±0.09	0.38±0.52	<0.05
T1W-BB	AS	939.37±266.33	139.40±198.16	<0.05
	SI	2.55±0.72	0.46±0.64	<0.05

IMH, intramural haematoma; SNAP, simultaneous non-contrast angiography and intraplaque haemorrhage; T1W-BB, T1-weighted black blood imaging; AS, absolute signal; SI, signal index.

months later (Table 1, Fig 2). Comparing with the initial examination, the AS and SI of IMH of vessel wall images within SNAP and T1W-BB sequence decreased significantly at 3 months after treatment ($p<0.05$; Table 2, Fig 2). The SNR of IMH of vessel wall images within the SNAP sequence was significantly higher than T1W-BB, T2W-BB, PD-VISTA sequences ($p<0.05$; Table 3, Fig 3).

Discussion

Conventional vascular imaging techniques for analysis of intracranial vascular disease provide limited information as

Table 3

Comparison of the SNR of the IMH between vessel wall images using SNAP and other sequences (mean±standard deviation).

	SNAP	PD-VISTA	SNAP	T1W-BB	SNAP	T2W-BB
SNR	113.28±81.30	10.52±5.95	113.28±81.30	15.32±5.60	113.28±81.30	8.53±4.97
p-Value	<0.05		<0.05		<0.05	

IMH, intramural haematoma; SNAP, simultaneous non-contrast angiography and intraplaque haemorrhage; PD-VISTA, proton-density-weighted volume isotropic turbo spin-echo acquisition imaging; T1W-BB, T1-weighted black blood imaging; T2W-BB, T2 weighted black blood imaging; SNR, signal-to-noise ratio.

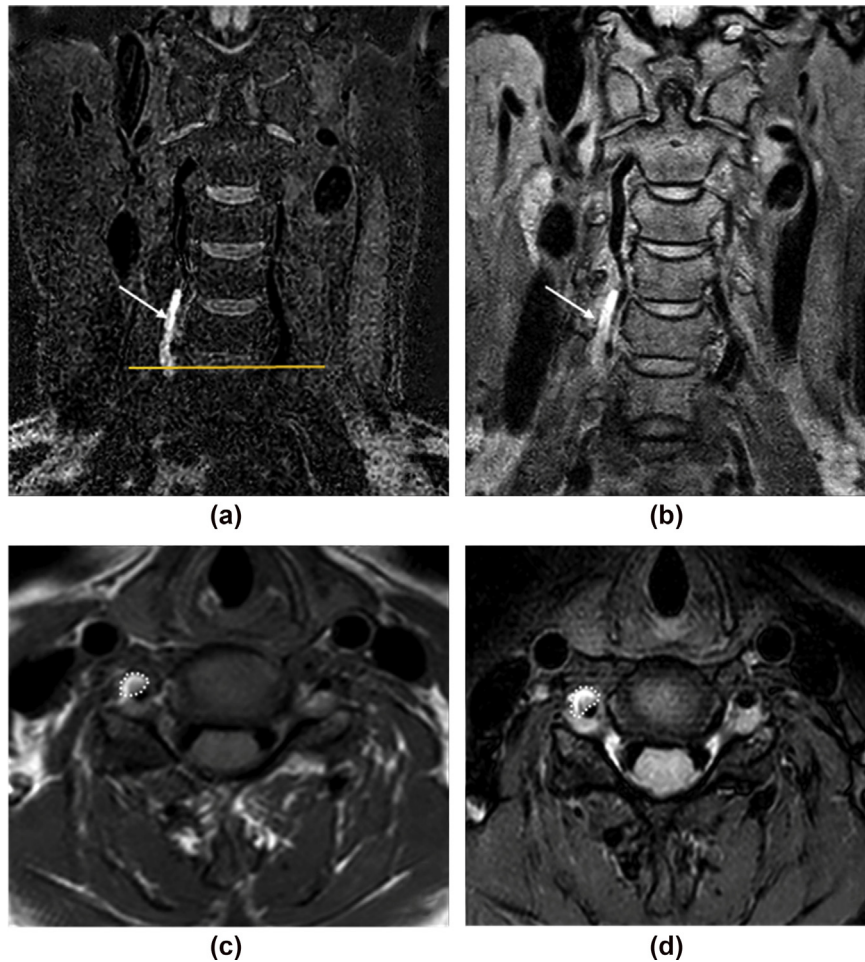


Figure 3 A 40-year-old female patient with right vertebral artery (RVA) dissection. IMH was best displayed on the vessel wall image within (a) SNAP (arrow) with clear range, while the signal from the IMH was partially similar to the surrounding tissue on PD-VISTA (b, arrow), T1W-BB (c, dotted area), and T2W-BB images (d, dotted area) (Transverse image was obtained at the level of transverse line.).

they only identify changes to the vessel lumen.¹⁹ HRMRI was recently introduced and used to visualise the lumen and the types of vessel wall lesions of intracranial arteries. In intracranial artery dissection, HRMRI, which includes 3D FS T1W images with a BB effect, is regarded as the optimal diagnostic technique.¹⁰ T1-VISTA imaging sequence has a high display rate for CeAD signs, such as intimal flaps, IMH, and dilatations.²⁰

CVUS is sensitive to CeAD, which is often shown as IMH and tearing intimal flaps. Over other angiographic examinations, US has the diagnostic advantages of direct view, accuracy, and low cost.⁶ Duplex US distinctly depicts intramural haematomas. Thus, US has been the reference imaging in the clinical assessment of patients suspected of having CeAD. In addition, US can display other significant signs of CeAD, such as a tear in the intimal flap and thrombosis in the lumen,⁶ but it also has some shortcomings, such as limited value of arteries covered by the skull or vertebral body. In addition, CVUS is currently mainly used as the first-line screening method for cervical vascular diseases. For patients without typical signs of CeAD, further conventional HRMRI examination is still needed.

Long acquisition times can increase the probability of motion artefacts due to swallowing, respiration, or neck movements.²¹ It is likely to be more serious for CeAD patients because they are more unbearable for long scan time because of pain and ischaemic symptoms. The SNAP imaging technique can detect both luminal stenosis and IMH with a single scan. The scanning time of the SNAP sequence was about half that of 3D TOF MRA plus the T1W-BB sequence. By using phase-sensitive reconstruction, the SNAP technique was optimised so that the luminal signal was always present as a negative signal while the IMH was always present as a strong positive signal.¹⁴ This not only reduces scanning time, but also improves the detection rate of IMH. Several studies show that unenhanced MRA images derived from SNAP imaging had excellent agreement with 3D TOF MRA as well as contrast-enhanced MRA in evaluating luminal stenosis.^{9,12,15} For the diagnosis of aetiology, SNAP has been applied to the diagnosis of intraplaque haemorrhage (IPH)^{14,15} as well as IMH.⁹ Recently, SNAP has been used to characterise the surface of the plaque.¹¹ The present findings are consistent with those of previous studies. Using 3D Multi-Echo Recombined Gradient Echo (MERGE) images as the reference standard, Li *et al.*⁹ demonstrated that SNAP had excellent agreement with conventional HRMRI in the evaluation of luminal stenosis and IMH in patients with CeAD. In the present study, conventional sequences and CVUS were used as controls, which optimised the evaluation of SNAP for IMH identification. The present study indicates that SNAP has high sensitivity and specificity for the diagnosis of CeAD, with high coherence with conventional sequences as well as CVUS and much shorter scanning time compared with conventional sequences. The SNAP sequence still needs further verification to become a first-line examination method for CeAD in the future.

On analysis of the AS and SI, both the SNAP and T1W-BB sequences could reflect the absorption of IMH after

treatment. There was no significant difference between the AS or SI of IMH of vessel wall images between the SNAP and T1W-BB sequences during review, while both the AS and SI between vessel wall images within the SNAP sequence and T1W-BB sequence had significant differences during the initial examination, which suggested that these two sequences had similar value in the evaluation of IMH after treatment.

In addition to identifying the feasibility of the SNAP sequence in the diagnosis of IMH, the SNAP sequence was found to have a higher SNR compared to the T1W-BB sequence, indicating that the SNAP sequence could display IMH better and improve confidence in the diagnosis of CeAD.

The present study has several limitations. First, the sample size was small, which may affect the accuracy of the SNAP sequence in the diagnosis of CeAD, and further prospective studies with larger sample sizes are warranted. Second, conventional sequences were used for validation of SNAP imaging in evaluation of CeAD, but validation of SNAP imaging using catheter angiography in future studies is warranted. Third, the display rates of the signs using the different methods were not recorded. Finally, deviation of AS and SI may exist in manual measurement.

In conclusion, the SNAP technique showed great promise for imaging of IMH. With its large coverage, high resolution, and simultaneous MRA/IMH images, the SNAP sequence might be an alternative, time-efficient diagnostic tool for characterisation of CeAD.

Conflict of interest

The authors declare no conflict of interest.

Acknowledgements

This work was supported by the National Natural Science Foundation of China (grant number 81671743) and Clinical Key Diseases Diagnosis and Therapy Special Foundation of Suzhou City, China (grant number LCZX201801).

References

- Shakir HJ, Davies JM, Shallwani H, *et al.* Carotid and vertebral dissection imaging. *Curr Pain Headache Rep* 2016;**20**(12):68.
- Debette S, Leys D. Cervical-artery dissections: predisposing factors, diagnosis, and outcome. *Lancet Neurol* 2009;**8**(7):668–78.
- Robertson JJ, Koyfman A. Cervical artery dissections: a review. *J Emerg Med* 2016;**51**(5):508–18.
- Yamada S, Ohnishi H, Takamura Y, *et al.* Diagnosing intra-cranial and cervical artery dissection using MRI as the initial modality. *J Clin Neurosci* 2016;**33**:177–81.
- Benninger DH, Baumgartner RW. Ultrasound diagnosis of cervical artery dissection. *Front Neurol Neurosci* 2006;**21**:70–84.
- Yang L, Ran H. Extracranial vertebral artery dissection: findings and advantages of ultrasonography. *Medicine* 2018;**97**(9):e0067.
- Woo KJ, Na-Young S, Dae KY, *et al.* Added value of 3D proton-density weighted images in diagnosis of intracranial arterial dissection. *PLoS ONE* 2016;**11**(11):e0166929.
- Kinoshita T, Ogawa T, Kado H, *et al.* CT angiography in the evaluation of intracranial occlusive disease with collateral circulation: comparison with MR angiography. *Clin Imaging* 2005;**29**:303–6.

9. Li Q, Wang J, Chen H, et al. Characterization of craniocervical artery dissection by simultaneous MR noncontrast angiography and intraplaque haemorrhage imaging at 3 T. *ANJR Am J Neuroradiol* 2015;**36**(9):1769.
10. Hwang J, Chung JW, Cha J, et al. Selective application of high-resolution 3 T MRI in the evaluation of intracranial vertebral artery dissection. *J Neuroimaging* 2016;**27**(1):71–7.
11. Chen S, Zhao H, Li J, et al. Evaluation of carotid atherosclerotic plaque surface characteristics utilizing simultaneous noncontrast angiography and intraplaque haemorrhage (SNAP) technique. *J Magn Reson Imaging* 2017. 00: 000-000.
12. Chen S, Ning J, Zhao X, et al. Fast simultaneous noncontrast angiography and intraplaque haemorrhage (fSNAP) sequence for carotid artery imaging. *Magn Reson Med* 2017 Feb;**77**(2):753–8.
13. Wang J, Guan M, Yamada K, et al. *In vivo* validation of simultaneous non-contrast angiography and intraplaque haemorrhage (SNAP) magnetic resonance angiography: an intracranial artery study. *Plos One* 2016;**11**(2):e0149130.
14. Wang J, Börnert P, Zhao H, et al. Simultaneous noncontrast angiography and intraplaque haemorrhage (SNAP) imaging for carotid atherosclerotic disease evaluation. *Magn Reson Med* 2013;**69**(2):337–45.
15. Shu H, Sun J, Hatsukami TS, et al. Simultaneous noncontrast angiography and intraplaque haemorrhage (SNAP) imaging: comparison with contrast-enhanced MR angiography for measuring carotid stenosis. *J Magn Reson Imaging* 2017;**46**(4):1045.
16. Choi YJ, Jung SC, Lee DH. Vessel wall imaging of the intracranial and cervical carotid arteries. *J Stroke* 2015;**17**(3):238–55.
17. Park KJ, Jung SC, Kim HS, et al. Multi-contrast high-resolution magnetic resonance findings of spontaneous and unruptured intracranial vertebral artery dissection: qualitative and quantitative analysis according to stages. *Cerebrovasc Dis* 2016;**42**:23–31.
18. Akmal S, Zhonghua S, Yusof AKM. Coronary CT angiography with single-source and dual-source CT: comparison of image quality and radiation dose between prospective ECG-triggered and retrospective ECG-gated protocols. *Int J Cardiol* 2013;**168**(2):746–53.
19. Alexander MD, Yuan C, Rutman A, et al. High-resolution intracranial vessel wall imaging: imaging beyond the lumen. *J Neurol Neurosurg Psychiatr* 2016;**87**(6):589.
20. Sakurai K, Miura T, Sagisaka T, et al. Evaluation of luminal and vessel wall abnormalities in subacute and other stages of intracranial vertebral artery dissections using the volume isotropic turbo-spin-echo acquisition (VISTA) sequence: a preliminary study. *J Neuroradiol* 2013;**40**(1):19–28.
21. Balu N, Yarnykh VL, Chu B, et al. Carotid plaque assessment using fast 3D isotropic resolution black-blood MRI. *Magn Reson Med* 2011;**65**(3):627–37.